Efficient analysis methodologies for emerging oscillator configurations

Almudena Suárez
Ingeniería de Comunicaciones
Universidad de Cantabria
Santander, Spain
almudena.suarez@unican.es

***Abstract*— Oscillators enable a low-cost and compact implementation of radio-frequency identification (RFID) readers and radar systems, among other. The function integration comes at the cost of a more complex performance and a demanding analysis since the circuit must respond to several specifications, while maintaining the oscillation condition. Here a review of recently introduced semi-analytical formulations, intended for these oscillator-based circuits, is presented. They are based on the use of a numerical model of the standalone oscillator, extracted from harmonic-balance or envelope-transient simulations, which is introduced in an analytical description of the oscillator interaction with the external elements. Various types of formulations, applied to self-injection locked radar, RFID readers and super-regenerative oscillators, will be described and validated.**

Keywords—Nonlinear circuit analysis, self-injection locked oscillator, hysteresis, super-regenerative oscillator

I. INTRODUCTION

As recently shown [1]-[6], oscillator circuits enable a compact and low-cost implementation of RFID readers and radar systems, among other. This is obtained through the combination of the inherent carrier generation with other functions, such as frequency modulation or mixing. However, this function integration comes at the cost of a more complex performance and a demanding analysis, since the circuit must respond to several specifications, while maintaining the oscillation condition. Furthermore, the interaction with external elements often induces multivalued sections in the oscillator solution curves, as well as unstable behavior [5].

In self-injection-locked radar [1] and oscillator-based RFID readers [2], the oscillation signal is transmitted and reinjected into the same oscillator circuit after undergoing the effect of external elements. As shown here, their behavior can be efficiently analyzed by means of semi-analytical formulations [3]-[5], which enable a compromise between accuracy and insight. They are based on a numerical model of the standalone oscillator, extracted from harmonic balance (HB) and introduced in an analytical description of the oscillator interaction with the external elements. This provides insight into the effect of the various elements, including the main oscillator characteristics, on the overall system response.

Super-regenerative oscillators (SROs) [7], switched on and off by a quench signal, take advantage of the initial exponential growth of an oscillation to obtain high gain amplification in a compact manner. They can also be used as active transponders, since they provide an amplified signal that is approximately phase-coherent with the interrogating one [6]. Their behavior of SROs is conceptually complex and involves two distinct time scales, corresponding to the oscillation and the quench signal. They are usually described with idealized oscillator models, which limits the analysis prediction capabilities. As shown here, a realistic prediction is enabled by a semi-analytical model based on a black-box linear time-variant transfer function [8] in the envelope domain. This can be used to obtain the SRO response to arbitrarily modulated input signals in an efficient manner.

II. SELF-INJECTION LOCKED OSCILLATORS

A. Self-injection locked radar

As shown in [1], self-injection-locked radar can be efficiently used for person localization and breathing-rate measurement. In standalone conditions, the oscillator fulfils $Y(V_o,\omega_o) = 0$, where Y is the current-to-voltage ratio and ω_o and V_o are oscillation frequency and amplitude at the output port. In self-injection locked operation, the oscillator signal is transmitted, partially reflected by the target, and reinjected into the oscillator. Under a single antenna of gain G, the reflection coefficient seen from the antenna terminals is [9]:

$$\Gamma(G,d,\omega) = \frac{G\lambda}{d^2}\sqrt{\frac{\sigma}{(4\pi)^3}}e^{-j\omega\frac{2d}{c}} = \frac{A_o G}{d^2\omega}e^{-j\omega\frac{2d}{c}} \qquad (1)$$

where d is the distance to the target, σ is the radar cross section and c is the speed of light. The corresponding load admittance is $Y_L = Y_o(1-\Gamma)/(1+\Gamma)$. For the usually high attenuation values, one can approach $Y_L \cong Y_o(1-2\Gamma)$. The change $\Delta Y_L = Y_L - Y_o$ in the load admittance will induce variations in the oscillation amplitude and frequency [5]. Assuming that these variations are small (due the attenuation effects), the oscillator semi-analytical equation is:

$$Y_V(V-V_o) + Y_\omega(\omega-\omega_o) - 2Y_o\frac{A_o G}{d^2\omega_s}e^{-j\omega\frac{2d}{c}} = 0 \qquad (2)$$

where Y_V and Y_ω are the derivatives of the oscillator admittance about the free-running point. Note that the load admittance increment is not linearized due to the strong phase variations. The derivatives Y_V and Y_ω can be easily extracted from harmonic balance (HB). This is done by (i) introducing an auxiliary generator at the output of the standalone oscillator, which must exhibit zero value of its current-to-voltage ratio ($Y = 0$), and (ii) applying finite differences to V and ω [5]. From the inspection of (2), one can expect multivalued solutions under relatively high G due to the complex exponential [5]. Assuming a slow target motion, as in the detection of biomedical signals, one will have the distance $d + x(t)$, and the system will be governed by:

$$Y_V\left(V(t)-V_o\right) + Y_\omega\left(\omega(t)-\omega_o\right) - 2Y_o\frac{A_0 G}{d^2\omega_s}e^{-j\omega\left(\frac{2d+2x(t)}{c}\right)} = 0 \qquad (3)$$

where the time derivatives of the amplitude and phase are neglected due to the slow variation of $x(t)$. The method has been applied to transistor-based (NE3210S01) oscillator at 2.4 GHz [5]. Fig. 1(b) presents a comparison between the analysis and measurement results for $d = 0.45$ m and a periodic target motion with an excursion of 1 cm at 2.7 Hz.

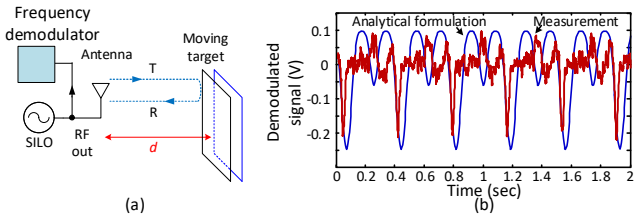

Fig. 1. Self-injection-locked radar. (a) Schematic. (b) Demodulated signal under the target motion. Comparison between analysis and measurements.

B. *RFID systems*

The work [2] proposed a compact RFID reader of chipless tags, based on a chirped oscillator [Fig. 2(a)]. The oscillator frequency must cover the whole interval of the tag resonances [2], which is achieved introducing a low-frequency sawtooth in the bias line. When the oscillator is placed near the tag, its instantaneous frequency is affected by the tag resonators. Then, the tag signature is recovered from the voltage drop in a bias resistor [2], which varies with the oscillation frequency. Under the effect of the sawtooth signal $\eta(t)$ and the chipless tag [3], the oscillator semi-analytical equation is:

$$Y_V(\eta)\Delta V(t)+Y_\omega(\eta)\left[\dot{\phi}(t)-j\frac{\Delta\dot{V}(t)}{V_o(\eta)+\Delta V(t)}\right]=\frac{-\Delta y_{L,lp}(t)*X_1(t)}{X_1(t)} \quad (4)$$

where $X_1(t)\equiv\left[V_o(\eta)+\Delta V(t)\right]e^{j\phi(t)}$ and $\Delta y_{L,lp}(t)$ is the lowpass impulse response associated with the increment of the oscillator load admittance $\Delta Y_{L,lp}(\omega)$.

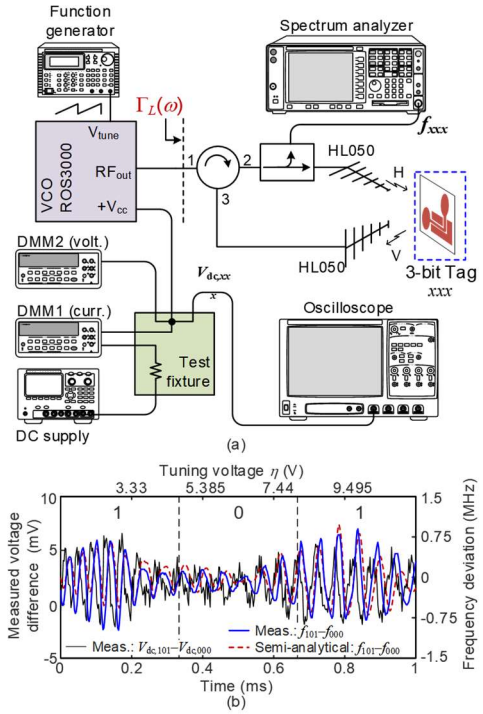

Fig. 2 Oscillator-based RFID reader. (a) Set-up. (b) Simulated and measured difference between the detected signals for 101 and 000.

Equation (4) has two key differences with (1): it requires obtaining the functions $Y_V(\eta)$ and $Y_\omega(\eta)$, and the time derivatives of the oscillation frequency and amplitude, resulting from the effect of the sawtooth signal, cannot be neglected. To calculate $Y_V(\eta)$ and $Y_\omega(\eta)$ one should sweep η, and, at each η step, obtain the new steady-state solution (fulfilling $Y=0$) and then, the derivatives through finite differences. When using a commercial oscillator, the derivatives can be obtained experimentally through the procedure in [3]. Equation (4) is solved through integration in the envelope domain. It has been applied to a system based on a ROS3000 under a sawtooth of 1 kHz and a retransmission tag [20] that contains three coplanar waveguide spiral resonators [Fig. 2(a)], each corresponding to a coding bit. Fig. 2(b) presents the differences in the simulated and measured demodulated signal when using the signature 101 and the signature 000.

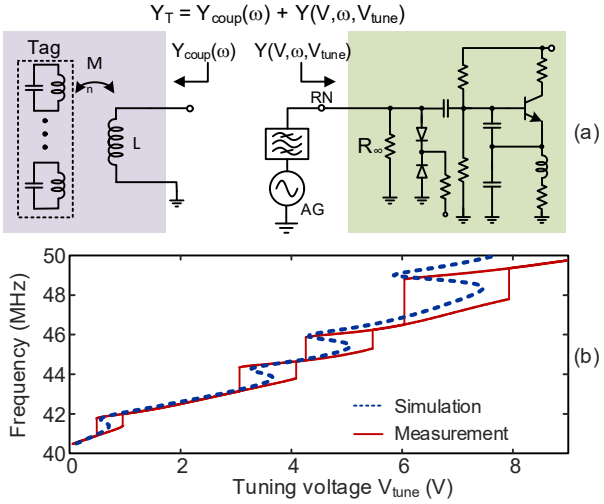

Fig. 3 RFID application based on the oscillator coupling to several external resonators. (a) Schematic. (b) Analysis and measurement results.

An implementation based on resonator magnetic coupling has also been investigated [4], in which the oscillator sensitivity to the tag resonances can be increased by inducing hysteresis cycles in the oscillator characteristic versus the tuning voltage η. The concept departs from the so-called "dip oscillator" [10], which undergoes an amplitude change when weakly coupled to a passive resonator, tuned to its free-running frequency. As shown in [4], from a certain value (still relatively small) of the coupling factor k, hysteresis is obtained versus the tuning voltage η. This gives rise to a physical jump in the oscillator frequency and amplitude, and, thus, to a very noticeable response to the external resonator. In the RFID application [11], the tag will contain N resonators tuned at distinct frequencies ω_n, comprised in the oscillation frequency interval versus η. Under small coupling factors, the oscillator is approximately described with:

$$Y(V,\omega,\eta)+\frac{1}{jL\omega}+\sum_{n=1}^{N}\frac{M_n^2}{L^2}\frac{1}{R_n+jL_n\omega+\frac{1}{jC_n\omega}}=0 \quad (5)$$

where $M_n=k_n\sqrt{LL_n}$, and L is the coupled oscillator inductor. Unlike the previous formulations, (5) uses a nonlinear function $Y(V,\omega,\eta)$ to represent the oscillator admittance. Note that the inductor admittance must be subtracted since it is considered in the coupled term. The function $Y(V,\omega,\eta)$ is obtained with HB by means of a triple sweep in V,ω,η. For each η, the solutions of (5) are calculated in in-house software from the intersections of the contours $\mathrm{Re}\left[Y(V,\omega,\eta)\right]=0$ and $\mathrm{Im}\left[Y(V,\omega,\eta)\right]=0$. When varying η, there can be three solutions of (5) about the value that

provides ω_n in standalone operation, which is due to the form of variation of the additional term resulting from the coupled resonators. Thus, provided a suitable design is carried out, there will be a small hysteresis cycle versus η about each ω_n. This can be seen in Fig 3(b), where four coupled resonators have been considered, which, in the measured results, give rise to four physical jumps. One can encode a particular bit pattern by activating or deactivating the resonators in the coupled tag. As in the previous case, the reading mechanism involves the use of sawtooth signal [4].

III. Super-regenerative oscillators

Super-regenerative oscillators [7] are switched on and off by a low-frequency quench signal [Fig. 4(a)]. They take advantage of the fast growth of the oscillation amplitude during the start-up transient to provide high gain amplification of input signals at frequencies near the oscillation one. During each quench period, the dominant pair of complex-conjugate poles of the dc solution (at the oscillation frequency) shifts from the left-hand side (LHS) of the complex plane to the right-hand side (RHS) and then back to the LHS. The SRO operation involves two time scales, corresponding to the quench and oscillation signals, so an envelope-domain analysis is well suited, as shown in [6]. When the oscillation is quenched before reaching the nonlinear transient stage, the SRO response to an arbitrarily modulated small-signal input can be obtained from a linear-time-variant (LTV) transfer function $H(t, \omega)$. This is calculated exciting the circuit with a small-signal *sinusoidal* source [Fig. 4(b)] at the frequency ω. This frequency is swept and a circuit-level envelope-transient analysis is carried out at each ω to obtain $H(t,\omega) = V_{out}(t,\omega)/V_{in}$, where $V_{out}(t,\omega)$ is the envelope of the output-signal [Fig. 4(b)]. Then, under an arbitrarily modulated input signal, with the envelope $V_{in}(t)$, the envelope of the output signal is given by [6]:

$$V_{out}(t) = \frac{1}{2\pi}\int_{-B/2}^{B/2} H(t,\Omega+\omega_p)V_{in}(\Omega)e^{j\Omega t}d\Omega \qquad (6)$$

The use of (6) avoids the need to perform any new circuit-level simulations when changing $V_{in}(t)$. The method has been applied to a transistor-based SRO at 2.7 GHz in Fig. 5(a), with the quench frequency f_q = 8 MHz, under an on-off keying modulation [Fig. 5(b)] at f_{mod} = 800 KHz. Results have been successfully compared with circuit-level envelope-domain simulations and measurements [Fig. 5(c)].

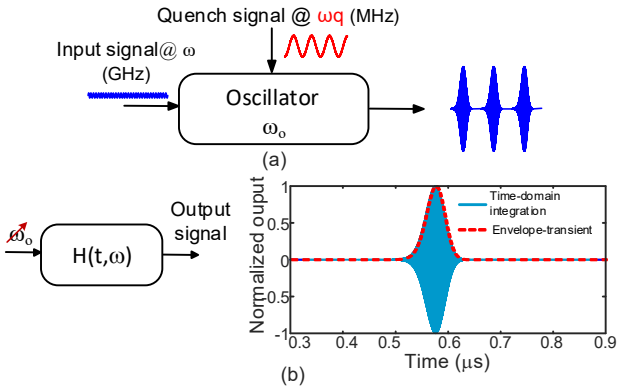

Fig. 4 Super-regenerative oscillator. (a) Operation concept. (b) Calculation of the LTV transfer function $H(t, \omega)$ through circuit-level envelope transient.

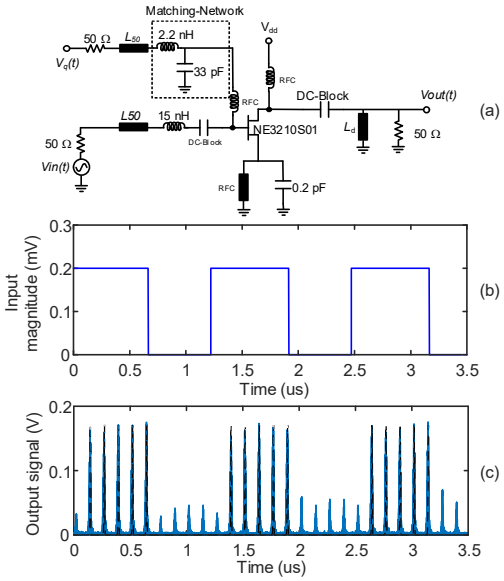

Fig. 5. Super-regenerative oscillator. (a) Schematic. (b) Input-signal envelope. (b) Output-signal envelope. Comparison with circuit-level envelope-domain simulations (overlapped) and measurements.

Conclusions

A review of different types of semi-analytical formulations enabling a realistic and efficient analysis and design of emerging oscillator configurations for RFID readers and radar systems has been presented.

Acknowledgment

Author is grateful to S. Sancho, F. Ramírez and M. Pontón, from U. of Cantabria, R. Melville from Emecom, and S. Hernandez from AMCAD Engineering. Work supported by project TEC2017-88242-C3-1-R (AEI,FEDER/UE).

References

[1] S. H. Yu and T. S. Horng, "Highly Linear Phase-Canceling Self-Injection-Locked Ultrasonic Radar for Non-Contact Monitoring of Respiration and Heartbeat," *IEEE Trans. Biomed. Circuits Syst.*, vol. 14, no. 1, pp. 75–90, Feb. 2020.

[2] N. B. Buchanan, V. Fusco, "Single VCO chipless RFID near-field reader," *Elect. Lett.*, vol. 52, no. 23, pp. 1958-1960, 11 10 2016.

[3] F. Ramírez, S. Sancho, M. Pontón, A. Suárez, "Two-Scale Envelope-Domain Analysis of Injected Chirped Oscillators," *IEEE Trans. Microw. Theory Techn.*, vol. 66, no. 12, pp. 5449-5461, Dec., 2018.

[4] A. Suarez, R. Melville, and F. Ramirez, "Analysis and Synthesis of Hysteresis Loops in an Oscillator Frequency Characteristic," *IEEE Trans. Microw. Theory Tech.*, vol. 67, no. 12, 2019.

[5] M. Pontón, A. Suárez, "Wireless Injection Locking of Oscillator Circuits," *IEEE Trans. Microw. Theory Tech.*, vol. 64, no. 12, pp. 4646-4659, Dec. 2016

[6] S. Hernández and A. Suárez, "Envelope-Domain Analysis and Modeling of Super-Regenerative Oscillators," *IEEE Trans. Microw. Theory Tech.*, vol. 66, no. 8, pp. 3877-3893.

[7] F. X. Moncunill-Geniz, P. Pala-Schonwalder and O. Mas-Casals, "A generic approach to the theory of superregenerative reception," *IEEE Trans. Circuits Syst. I, Reg. Papers*, vol. 52, no. 1, pp. 54-70, Jan. 2005.

[8] C. Carlowitz and M. Vossiek, "Demonstration of an efficient high speed communication link based on regenerative sampling," *2017 IEEE MTT-S Int. Microwave Symposium (IMS)*, Honolulu, HI, 2017, pp. 71-74.

[9] B.Jang, *et. al*, "Wirelesss Bio-Radar Sensor for Heartbeat and Respiration Detection," *Prog. Electromagn. Res.*, vol. 5, pp. 149–168, 2008.

[10] *The Amateur Radio Handbook*, Third Ed., Radio Society of Great Britian, 28 Little Russel St, (1961), London, W.C.1, pp. 473-476.

[11] S. Preradovic, I. Balbin, N. C. Karmakar, G. F. Swiegers, "Multiresonator-Based Chipless RFID System for Low-Cost Item Tracking," *IEEE Trans. Microw. Theory Techn.*, vol. 57, no. 5, pp. 1411-1419, May 2009.